

STRIPE PHASES IN HIGH-TEMPERATURE SUPERCONDUCTORS*

ANDRZEJ M. OLEŚ

Institute of Physics, Jagellonian University
Reymonta 4, 30-059 Kraków, Poland
e-mail: amoles@if.uj.edu.pl

(Received November 14, 2000)

We review recent results obtained for the stripe phases in the Hubbard model. The experimentally observed half-filled (01) stripes with the filling of one hole per two domain wall atoms are stabilized by electron correlation effects. We show that the metallic stripe phases obtained using the dynamical mean-field approximation are stabilized by a pseudogap and are qualitatively different from insulating stripes derived from the one-particle (Hartree–Fock) simulations. They reproduce the doping dependence of the size of magnetic domains in (01) stripe phases and agree with the experimental data of angle resolved photoemission for $\text{La}_{2-x}\text{Sr}_x\text{CuO}_4$.

PACS numbers: 74.72.-h, 71.27.+a, 79.60.-i, 71.10.Fd

1. Mott insulators and stripe phases

Numerous fascinating phenomena, such as various types of competing magnetically ordered phases, metal-insulator transitions, and high-temperature superconductivity observed in transition metal oxides, are caused by the collective behavior of strongly correlated electrons [1]. It was recognized first by Mott that the large local electron–electron interaction U might dominate over the kinetic energy $\propto t$, and could cause electron localization in a half-filled band with electron density $n = 1$ per atom, thus explaining a new type of insulating state, the so-called Mott insulator [2]. In this state part of the degrees of freedom is removed, as the charge fluctuations are suppressed, and the problem of fermions on a lattice reduces to the spin problem, in the simplest case described by the Heisenberg model with a nearest-neighbor antiferromagnetic (AF) kinetic exchange interaction

* Presented at the XL Cracow School of Theoretical Physics, Zakopane, Poland June 3–11, 2000.

$J > 0$. Therefore, if no other degree of freedom is present and the lattice is nonfrustrated, Mott insulators have an AF long-range order in the ground state. Such a state would be stable on a three-dimensional cubic lattice, realized by the transition metal oxides with perovskite structures, but frequently further complications such as orbital degeneracy occur, leading to the effective interactions that are more difficult to describe, and may favor qualitatively new magnetic states [3]. Fortunately, the parent compounds of the High-Temperature Superconducting Oxides (HTSO), such as La_2CuO_4 and $\text{YBa}_2\text{Cu}_3\text{O}_6$, are simpler — they have CuO_2 planes as a common structural element, well separated from all other ions due to large lattice distortions, and orbital degeneracy is removed. Such planes can be described by an effective two-dimensional (2D) model of electrons interacting on a square lattice, the Hubbard model.

In addition to the Mott insulating state itself, a more difficult and challenging subject has been to describe and understand correlated metallic phases near the Mott insulator. In this regime the charge fluctuations occur in addition to the spin fluctuations, and give rise to the anomalous metallic phase [4]. Such a situation occurs for instance in $\text{La}_{2-x}\text{Sr}_x\text{CuO}_4$, where the doping by divalent Sr ions decreases the electron density to $n = 1 - x < 1$, and holes doped to an antiferromagnet can move only in a restricted space, defined by the constraint of no double occupancy due to large U . In HTSO this metallic phase is unstable in a very spectacular way — the system becomes superconducting at low temperature. Here we will not address the central and outstanding question concerning the mechanism of superconductivity, but discuss the qualitatively new phenomenon which occurs in the normal phase — the instability towards a novel type of charge and magnetically ordered state, the so-called *stripe phase* [5].

As one of very few predictions in the theory of high temperature superconductivity, the stripes were found in Hartree–Fock (HF) calculations on finite lattices described by the Hubbard model [6], well before their experimental confirmation [7]. Such states result from the competition between the superexchange interactions $\propto J = 4t^2/U$ (t is here an effective parameter for the Cu–Cu hopping which may be derived from the realistic charge-transfer model, where a more quantitative analysis of the superexchange J is possible [8]), which stabilizes the AF long-range order in the undoped materials [9], and the kinetic energy of holes $\propto t$ which are doped to this AF state. This physical situation is described by the effective Hamiltonian, the so-called t – J model, derived many years ago [10] and now used for a generic description of the phenomena in doped AF insulators, *inter alia* also for the holes moving in doped CuO_2 planes [11]. On one hand, the magnetic energy is gained when the electrons occupy the neighboring sites and the spins order as in the Néel state, while on the other hand, the holes can move much easier

when the AF order is suppressed, at least locally in this part of a CuO_2 plane where the holes are moving. In the extreme case when the local Coulomb interaction is very large $U \rightarrow \infty$, this leads to the polaronic mechanism of ferromagnetic (FM) order which is stabilized by a single hole/electron doped to a half-filled system, known as the Nagaoka theorem [12]. This case is special, as the magnetic interactions $\propto t^2/U$ vanish, and the kinetic energy is optimized in the FM phase. At large but finite U a compromise between these two energies has to be reached, and semiclassically they can be gained in different regions of a sample, with holons condensing in closed trajectories which gain the energy from quantum fluctuations [13]. This gives therefore a phase separation which manifests itself in a form of a stripe phase: the AF domains are separated by nonmagnetic lines, the one-dimensional (1D) domain walls. The kinetic energy is then best when the density of doped holes in a Domain Wall (DW) is large, and the AF domains are almost identical to the AF order in a Mott insulator [14, 15].

This phase separation into a stripe phase is very general and occurs in various transition metal oxides [1, 16]. The modulations in magnetization density have been detected in neutron scattering [7], and it was shown that they correspond to the AF domains separated by the DW's, qualitatively looking as those of Fig. 1. Here we will discuss the stripe phases only for HTSO, where static stripes were observed in $\text{La}_{1.6-x}\text{Nd}_{0.4}\text{Sr}_x\text{CuO}_4$ [7]. This subject is of great interest at present, and it is hoped that their investigations will help to understand the instabilities of doped Mott insulators, and the role of stripes in the high-temperature superconductivity. Arguments were given that the stripes suppress the superconductivity [17, 18], and indeed the static stripes occur only in the La-based compounds, where the transition temperature T_c is lower than in the Y- or Bi-based superconductors.

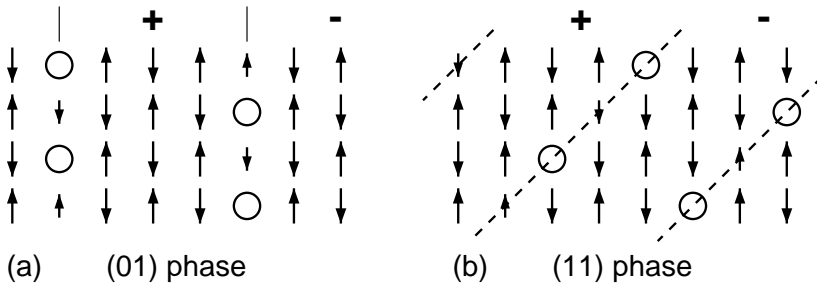


Fig. 1. Schematic structures of stripe phases with the filling of one hole per two DW's atoms (half-filled DW's) at doping $x = 1/8$: (a) (01) phase, and (b) (11) phase. Arrows stand for \uparrow - and \downarrow -moments in the stripe phase, with their length proportional to the local magnetization (3); circles indicate the positions occupied by holes. Two types of magnetic domains are indicated by + and -, respectively.

The stripe phases were obtained in HF calculations performed on the Hubbard model [6,19,20], t - J model [21], and more realistic charge-transfer models [22,23]. The most stable structures obtained in the HF approximation have the density of one doped hole per one atom in a DW, corresponding to *filled stripes* [20]. Such stripe phases were indeed observed in the nickelates [24]. On the contrary, it has been established experimentally in the cuprates that *one doped hole stabilizes two charge unit cells* in a stripe structure, *i.e.*, the magnetic states which form in CuO_2 planes of HTSO are *half-filled stripes*, with one hole per two DW atoms [7]. Two stripe phases with this filling and the magnetic unit cells consisting of 16 atoms, represented by two AF domains which are separated by two DW's with four holes in 8×4 clusters, corresponding to $x = 1/8$ doping, are shown schematically in Fig. 1. The picture is somewhat idealized, as the holes will partly delocalize in reality, and could also give equal densities and no magnetic moments at all DW atoms, as shown also by the numerical examples discussed in Secs. 3 and 5. The filled stripe phases would accommodate twice as many holes for the same cluster sizes and domain structures, and would correspond instead to $x = 1/4$ doping. It may be expected that the kinetic energy is quite different depending on the shape of magnetic domains and on the parameters of the microscopic model, and one has to determine the stable density and magnetization distributions in order to decide whether any of the two phases shown in Fig. 1, or any other phase, is the ground state configuration.

The above discrepancy between the theory and experiment shows that the classical instability is qualitatively incorrect in the cuprates, quantum fluctuations play an important role in stripe phases, and one is forced to go beyond the HF approximation, and treat explicitly *local electron correlations*. A few methods which include electron correlations, such as: the Density Matrix Renormalization Group (DMRG) for the t - J model [25], slave-boson mean field approach [26], variational wave functions described by the local ansatz [27,28], Exact Diagonalization (ED) of finite clusters [17], Monte-Carlo simulations applied to a spin-fermion model [29], analytic expansions of the wave function [30,31], Dynamical Mean-Field Theory (DMFT) [32], and cluster perturbation theory [33], have been used recently to investigate the stable ground states of stripe phases. It was a spectacular success of these methods that the half-filled stripe phases were obtained in all of them for the relevant parameters which model the HTSO.

The spectral properties of stripe phases are also of great interest, as the stripes have measurable consequences in photoemission [34–36]. If electron correlations are important, large corrections to the electronic structure, and to the gaps which stabilize the stripe phases in HF, are expected. It has been shown by recent numerical [17,33,37,38] and semianalytic [31] studies that the stripe superstructure induces drastic changes of the spectral weight dis-

tribution. Particularly intriguing are such observations as non-Fermi liquid dependence of the chemical potential on the doping [39], and the existence of a pseudogap which opens at the Fermi level in a broad regime of doping [36]. In addition, flat quasiparticle (QP) states have been observed near the $X = (\pi, 0)$ point in $\text{La}_{2-x}\text{Sr}_x\text{CuO}_4$ [36]. It will be shown that these features can be reproduced in the spectral functions obtained using an appropriate extension of the DMFT [40].

The rest of this paper is organized as follows. In Sec. 2 we present the microscopic reasons of stability of stripe phases in classical (HF) states and discuss the limitations of this approach. Better solutions can be obtained variationally, and we present in Sec. 3 an example of a variational wave function and show that it gives indeed stable half-filled stripes, with the same filling and orientation as observed experimentally. While this approach allows to investigate only the correlation energy and the structure of ground states, electron correlations are also important for the dynamical correlations seen in photoemission. They may be studied when a DMFT is generalized to the stripe phase [32], as presented in Sec. 4. Using this method, we analyzed in Sec. 5 the sequence of stable stripe phases with increasing hole doping x , and their spectral properties. The summary and some open problems related to stripe physics are presented in Sec. 6.

2. Solitonic mechanism of stripe formation

The realistic charge-transfer model for electronic states in CuO_2 planes of HTSO which includes $\text{Cu}(3d_{x^2-y^2})$ and $\text{O}(2p_{x(y)})$ orbitals may be replaced by a simpler effective Hubbard model which describes the interacting electrons on a square lattice occupied by Cu ions [41, 42],

$$H = - \sum_{mi,nj,\sigma} t_{mi,nj} a_{mi\sigma}^\dagger a_{nj\sigma} + U \sum_{mi} n_{mi\uparrow} n_{mi\downarrow}. \quad (1)$$

In the stripe phase the 2D square lattice is covered by N supercells containing L sites each. $a_{mi\sigma}^\dagger$ are creation operators for a hole at site $\{mi\}$, labeled by two indices: the supercell index m , and the index within the stripe unit cell $i = 1, \dots, L$, while $n_{mi\sigma} = a_{mi\sigma}^\dagger a_{mi\sigma}$ is the electron number operator. The usually discussed Hubbard model (1) includes only the hopping elements between nearest neighbors $t_{mi,nj} = t$, but in the superconducting cuprates it is derived from a realistic charge-transfer model, either by the cell method [41], or by the downfolding procedure, and therefore also finite hopping elements between second ($t_{mi,nj} = t'$) and third ($t_{mi,nj} = t''$) neighbors are of importance. The electrons interact by strong on-site Coulomb interaction $U \simeq 12t$.

In the HF approximation the interacting term is replaced by the potentials $\propto U$ which act on electron densities [6, 20]:

$$U n_{mi\uparrow} n_{mi\downarrow} \simeq U (\langle n_{mi\uparrow} \rangle n_{mi\downarrow} + n_{mi\uparrow} \langle n_{mi\downarrow} \rangle - \langle n_{mi\uparrow} \rangle \langle n_{mi\downarrow} \rangle). \quad (2)$$

The potentials consist of a nonmagnetic part $\propto U n_i$, where $n_i = \langle n_{mi\uparrow} + n_{mi\downarrow} \rangle$ is an electron density, and a magnetic part $\propto U m_i$, where

$$m_i = \langle n_{mi\uparrow} - n_{mi\downarrow} \rangle = 2 \langle S_i^z \rangle \quad (3)$$

is a local magnetization. Therefore, the electronic structure has to be solved self-consistently with local magnetic potentials, or *static selfenergy* [6],

$$\Sigma_{i\sigma}^{\text{HF}} = U n_{i\bar{\sigma}} = \frac{1}{2} U (n_i + \lambda_{\bar{\sigma}} m_i), \quad (4)$$

where $n_{i\bar{\sigma}} = \langle n_{mi\bar{\sigma}} \rangle$ with $\bar{\sigma} = -\sigma$ is the electron density in stripe supercell, and $\lambda_{\sigma} = \pm 1$ for $\sigma = \uparrow, \downarrow$. At half filling the electron density is uniform ($n_i = 1$), and the ground state is AF, with the magnetization $m > 0$ alternating between two sublattices A and B : $m_i = \pm m$ for $i \in A, B$. In the simplest case of $t' = t'' = 0$, the one-particle energy is given by $\varepsilon_{\mathbf{k}} = -2t(\cos k_x + \cos k_y)$, and the AF bands are easily obtained [43],

$$E_{\mathbf{k}}^{\pm} = \frac{1}{2} (\varepsilon_{\mathbf{k}} + \varepsilon_{\mathbf{k}+\mathbf{Q}}) \pm \frac{1}{2} [(\varepsilon_{\mathbf{k}} - \varepsilon_{\mathbf{k}+\mathbf{Q}})^2 + (Um)^2]^{1/2}, \quad (5)$$

where $\mathbf{Q} = (\pi, \pi)$ is the nesting vector in a 2D square lattice (*i.e.*, $\varepsilon_{\mathbf{k}+\mathbf{Q}} = -\varepsilon_{\mathbf{k}}$). Thus, if $U \gg t$, large potentials $\pm \frac{1}{2}U$ (4), defined with respect to the nonmagnetic uniform background, split the electronic structure (5) into occupied and empty states which are separated by a large gap $\sim U$, resulting in a Mott–Hubbard insulator. The AF subbands (5) simulate in the one-particle calculation the incoherent states of the Lower Hubbard Band (LHB) and Upper Hubbard Band (UHB) of a strongly correlated electron system [44], respectively.

The situation changes when holes are doped to an antiferromagnet. Consider first a single hole introduced by doping into an AF background [Fig. 2(a)]. If one spin is removed, one arrives at a many-body problem of a hole moving in an AF background which gives qualitatively new QP states accompanied by incoherent processes at higher energies [45]. In order to understand qualitatively the mechanism which favors stripes at higher doping, it is however enough to consider only a small cluster consisting of three atoms. This choice would be of course unrealistic for a single hole in an antiferromagnet, but in a stripe phase the symmetry is locally broken, and considering the (01) stripe phase of Fig. 1 one can first investigate the energy gain in the direction perpendicular to a DW itself. Thus, a cluster

consisting of three atoms and a hole in the middle is a simplest unit, representing either a line filled by holes in an antiferromagnet [Fig. 2(a)], or a hole on a DW, placed between two AF domains [Fig. 2(b)]. Thereby, we assume that the electrons cannot move due to large Coulomb interaction $U \gg t$, and thus the hole is confined only to the considered three atoms. If a \downarrow -spin is replaced by a hole in an antiferromagnet, as in Fig. 2(a), the situation in a resulting three-atom cluster is very simple — two \uparrow -spin electrons may be found in one of three possible configurations: $\{\uparrow 0 \uparrow\}$, $\{0 \uparrow \uparrow\}$, and $\{\uparrow \uparrow 0\}$, and thus this polaronic state gives the total energy

$$E_P = -\sqrt{2}t, \tag{6}$$

while the interaction energy U does not contribute.

If a hole occupies a DW instead, it may again delocalize over the molecular model of Fig. 2(b), which leads to similar three configurations to those considered for the polaron case: $\{\uparrow 0 \downarrow\}$, $\{0 \uparrow \downarrow\}$, and $\{\uparrow \downarrow 0\}$, but in addition, three configurations with one site doubly occupied, and three other configurations with the interchanged \uparrow - and \downarrow -spins, can be reached by the hole hopping. The latter configurations are accessible via double occupancies, and thus the energy can be found in a perturbative way. As a result, the energy is lower for this solitonic solution than in the polaronic case,

$$E_S = -\sqrt{2}t - \frac{4t^2}{U}. \tag{7}$$

Therefore, in the regime of large U , the DW is always more stable than a line of polarons in an AF background.

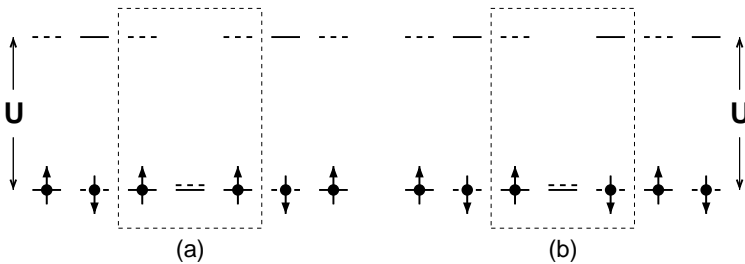


Fig. 2. Energy levels for the electrons with \uparrow -spin (full lines) and \downarrow -spin (dashed lines) in a 2D antiferromagnet along x axis: (a) a hole added to a single AF domain; (b) a hole on the DW separating two AF domains in (01) stripe phase. The spins form an AF structure, while the holes repeat themselves along y direction. Adding a second electron at an occupied site costs the Coulomb energy U .

In reality further corrections to the energies appear in both situations due to the interactions with the AF background, but the principal reason standing beyond the stripe formation is already identified by the above simple consideration [20]. If the holes occupy nonmagnetic DW's, additional processes are allowed in second order $\propto t^2/U$ which lower the energy of this structure with respect to the polaronic defects, where the analogous excitations are blocked by the Pauli principle. This also suggests that the (01) stripes are primarily stabilized by the hopping element perpendicular to the direction of the DW's. For this reason, (01) stripe structures can be additionally stabilized by lattice deformations which pin to the DW's, and give a nonperturbative renormalization of the second order energy gain of the solitonic solution (7), as analyzed in more detail in Ref. [20]. This result is counterintuitive, as naively one might expect that the doped holes fill a 1D band, with a dispersion

$$\varepsilon_{\mathbf{k}}^{\text{1D}} = -2t \cos k_y, \quad (8)$$

determined by the hopping along the DW direction [46], and this might decide about the stripe stability.

In order to understand why the stripes with filled DW's are more stable than those with half-filled DW's in the HF approach, it is instructive to investigate the electronic structure of a doped antiferromagnet. The bands are determined by the stable distribution of electron densities $\{n_{i\sigma}\}$ which give the HF potentials (4). While the magnetic potentials (4) are still present within the AF domains, and will thus give the electronic bands in the (occupied) LHB and in the (empty) UHB, these splittings are absent for the atoms on a nonmagnetic line which separates two AF domains. Therefore, a band which is built up mainly by the states of the DW atoms appears *within* a Mott–Hubbard gap [20]. This band is spin degenerate and may therefore accommodate two electrons per one atom of a DW. It cannot be filled by one electron per site, as then it would be again unstable against magnetic order, giving as a result a uniform AF phase of a Mott insulator, with the electronic structure considered above (5). On the contrary, if the DW is filled by holes, this band contains no electrons and is separated by a small gap $\propto t$ from the occupied states of the LHB. The Fermi energy μ lies in this gap, and in this way an insulating state with the filling of one doped hole per one DW atom is stabilized.

A very interesting question to ask now is whether any other than filled DW's might be stable in the HF approximation. The filling of one hole per two DW atoms, which was observed in the cuprates [7], corresponds to a quarter-filled band, which crosses the Fermi energy μ at $\mathbf{k} = (\pi, \pi/4)$, $(\pi/4, \pi/4)$, and other equivalent points. Therefore, such a state would be metallic and as such could not be even locally stable in HF. However, there

are still ways of stabilizing this filling by quadrupling of the unit cell along the DW's which opens a new gap in the quarter-filled band, precisely at the positions of the above crossing points. Indeed, when a spin-density wave (SDW) or a charge-density wave (CDW) with a periodicity of four atoms along the y direction is formed, such a gap opens at μ , and the stripes with half-filled DW's are locally stable [20]. Unfortunately, they can never be the most stable structures in HF for a very simple reason which can be understood by comparing the electronic structures of both types of stripe phases. In fact, the band which accommodates the doped holes splits into two almost flat subbands for the half-filled stripes, with either a SDW or a CDW along the DW's, and with almost no global shift of these subbands with respect to the center of the Mott–Hubbard gap. As only the upper subband is filled by holes, the total energy calculated per one doped hole is always higher in the half-filled stripe phase than that obtained when the DW is filled.

The observation that stable solutions are self-consistently obtained by placing the chemical potential μ in the middle of a gap gives a general mechanism of stripe phases in HF. Therefore, the stripe phases obtained in HF are always *insulating*. Recently, the electronic structures of different stripe phases were investigated in detail by Markiewicz [37]. Partial filling of the bands within the Mott–Hubbard gap and pseudogaps which form at the Fermi energy were found to be general consequences of stripe ordering, in qualitative agreement with the results of photoemission experiments [47]. However, the considered structures with partly filled DW's were only locally stable, similar for the stripes with half-filled DW's considered above. The same trend was also observed in the charge-transfer model [16].

Stripes may be seen as topological defects in an antiferromagnet, stabilized by the kinetic energy of doped holes. Their stability has a solitonic origin with nonmagnetic DW atoms, as shown both for small clusters [20], and for a 1D infinite system described by the Hubbard model [48]. Although no evidence was presented yet, it seems that the degeneracy of $3d$ orbitals might play a role in stabilizing the filled stripes in nickelates and manganese [1]. In contrast, orbital degeneracy is absent in the cuprates, and the quantum fluctuations for spins $s = \frac{1}{2}$ are expected to be larger than in other more classical compounds, where the spins are larger. In addition, also the electron correlation effects are particularly large in this case. We give arguments in the next Section that the analysis of the electronic structure alone cannot resolve the question of stripe stability and show that *electron correlations are responsible for stabilizing the half-filled stripes* in HTSO.

3. Variational wave functions

It is easy to understand why the electron correlations play such an important role in the physical properties of stripe phases. The HF approximation works well in the regime of large U only for the polarized (magnetic) states, and thus the correlation corrections are small for the atoms within the AF domains. The situation is quite different on the nonmagnetic DW's — here the correlation energy is large. Using the experience from the itinerant magnetism, where the correlation corrections are largest when the nonmagnetic atoms are close to half filling ($n = 1$) [49], it becomes clear that more correlation energy can be gained by reducing the double occupancy in the half-filled than in the filled stripe phases.

A variational treatment of the Hubbard model was first introduced by Gutzwiller, who formulated a systematic method of improving the HF wave function $|\Phi_0\rangle$ by implementing local correlations [50]. A recent extension of this method to the polaronic solutions and stripe phases has demonstrated that the half-filled DW's are stabilized by the correlation effects, and this trend is even more pronounced when the intersite Coulomb interactions are present [26]. Here the results of another approach which makes use of an exponential Local Ansatz (LA) for the correlated ground state [51],

$$|\Psi_0\rangle = \exp\left(-\sum_{mi} \eta_i O_{mi}\right) |\Phi_0\rangle, \quad (9)$$

will be discussed. This method captures the leading contribution to the correlation energy in the present systems with nonhomogeneous density distribution of doped holes. The local operators,

$$O_{mi} = n_{mi\uparrow}n_{mi\downarrow} - \langle n_{mi\uparrow} \rangle \langle n_{mi\downarrow} \rangle, \quad (10)$$

are introduced to reduce the amplitudes of the configurations with doubly occupied sites, and η_i are the corresponding variational parameters. The averages $\langle \dots \rangle$ are determined, as usually, by averaging over the HF ground state function $|\Phi_0\rangle$. By construction, the local operators describe the correlations which go *beyond* the HF state $|\Phi_0\rangle$, and $\langle O_{mi} \rangle = 0$. For convenience, we define the local doped hole and the local magnetization density at site $i = 1, \dots, L$ in the correlated ground state $|\Psi_0\rangle$ as follows,

$$n_{hi,LA} = \frac{\langle \Psi_0 | 1 - (n_{mi\uparrow} + n_{mi\downarrow}) | \Psi_0 \rangle}{\langle \Psi_0 | \Psi_0 \rangle}, \quad (11)$$

$$\langle S_i^z \rangle_{LA} = \frac{|\langle \Psi_0 | \frac{1}{2}(n_{mi\uparrow} - n_{mi\downarrow}) | \Psi_0 \rangle|}{\langle \Psi_0 | \Psi_0 \rangle}. \quad (12)$$

The breaking of symmetry is thereby assumed with respect to the z -th spin component, $S_{mi}^z = \frac{1}{2}(n_{mi\uparrow} - n_{mi\downarrow})$. This construction allows to use a closed-shell version of the HF wave function $|\Phi_0\rangle$ with the factorization of the Slater determinant into up-spin and down-spin parts.

The variational parameters $\{\eta_i\}$ are determined by minimizing the total energy in the correlated ground state,

$$E_0 = \frac{\langle \Psi_0 | H | \Psi_0 \rangle}{\langle \Psi_0 | \Psi_0 \rangle}. \quad (13)$$

After expanding the exponential factors in the wave functions $|\Psi_0\rangle$ (9) up to linear order in η_i , the stationary values of the variational parameters $\{\eta_i^0\}$ at the saddle point can be easily determined by minimizing the energy (13) [51]. The above procedure is valid provided that any third and higher order corrections, like $\propto \langle (n_{mi\uparrow} - \langle n_{mi\uparrow} \rangle)^3 \rangle$, are small and can be neglected [51]. This condition is well satisfied in the symmetry-broken states with AF order considered in the present study. More details on the energy minimization in the LA method may be found in Refs. [49] and [51].

The LA was used to investigate the stability of stripe phases by considering different starting density distributions and different topology of the DW's in finite 8×8 supercells with periodic boundary conditions [27]. Any self-consistent solution found in the variational LA is a local minimum of the total energy (13). Its absolute stability may be investigated by calculating the energy gain per one doped hole, as introduced in Ref. [20],

$$E_h^S(x) = \frac{1}{N_h} [E_0^S(x) - E_{AF}], \quad (14)$$

where N_h is the number of doped holes in the considered cluster. Here $E_0^S(x)$ is the energy obtained for the stable stripe phase at doping x , and E_{AF} is the reference energy of an undoped AF state in a Mott insulator (at $x = 0$), both found within the LA method.

The stripe phase, obtained as the ground state of a doped antiferromagnet by the above energy analysis, is characterized by the density (11) and magnetization (12) distribution. In the Hubbard model with the first neighbor hopping one finds (01) stripe phases as the lowest energy structures in a broad range of parameters [27]. For a (01) stripe phase with vertical DW's, one may label the atoms in the (magnetic) unit cell (which consists of a single row) by $l_x = 1, \dots, L$, while the atoms from different supercells are labeled by l_y , *i.e.*, a pair of indices $\{mi\}$ in Eq. (1) is here replaced by (l_x, l_y) . It is then more convenient to introduce the quantities integrated along the

direction parallel to the DW's [25]:

$$n_h(l_x) = 1 - \frac{1}{L_y} \sum_{l_y=1}^{L_y} \langle n_{(l_x, l_y), \uparrow} + n_{(l_x, l_y), \downarrow} \rangle, \quad (15)$$

$$S_\pi(l_x) = \frac{1}{L_y} \sum_{l_y=1}^{L_y} (-1)^{l_x+l_y} \frac{1}{2} \langle n_{(l_x, l_y), \uparrow} - n_{(l_x, l_y), \downarrow} \rangle, \quad (16)$$

where we have used the doped-hole density, $n_h(l_x) = 1 - \langle n_{(l_x, l_y), \uparrow} + n_{(l_x, l_y), \downarrow} \rangle$, instead of the local electron density $n_{(l_x, l_y)} = \langle n_{(l_x, l_y), \uparrow} + n_{(l_x, l_y), \downarrow} \rangle$, to characterize the stable charge distribution. A site-dependent factor $(-1)^{l_x+l_y}$ in Eq. (16) compensates the modulation of the AF structure within a single domain. Therefore, the charge and magnetization distribution in the (01) stripe phase is fully described by the average density along the (10) direction, given by $n_h(l_x)$ and $S_\pi(l_x)$, respectively. A similar procedure may be introduced to investigate the density and magnetization distribution in (11) stripe phases.

In the present paper we show for illustration the ground states obtained for hole doping $x = 1/8$ with two sets of parameters which were derived from the electronic structure [42]: (i) $t' = -0.11t$, $t'' = 0.04t$, and (ii) $t' = -0.30t$, $t'' = 0.20t$. They correspond to $\text{La}_{2-x}\text{Sr}_x\text{CuO}_4$ (LSCO) and $\text{YBa}_2\text{Cu}_3\text{O}_{6+x}$ (YBCO) compounds, respectively. In both cases the stripe structures have been found in the ground state. Although a stripe structure with magnetic DW's was found in HF for the LSCO parameters, a different (01) stripe phase with nonmagnetic DW's is obtained in the LA method [Fig. 3(a)]. This shows that the correlation energy gains are indeed larger for nonmagnetic atoms, and such solutions are stabilized when electron corrections are treated explicitly. This (01) phase is stable in a broad range of U , including $U \simeq 10t$ which is representative for LSCO compounds. It is expected that this phase will be stable also at $U > 10t$, as the obtained results are less reliable in this regime due to the performed expansion in $\{\eta_i\}$ parameters. Interestingly, a different stripe phase with diagonal (11) and FM DW's is more stable for the YBCO parameters [Fig. 3(b)]. This phase is clearly stabilized by a large second order hopping t' which leads to a kinetic energy gain when the spins are aligned within the walls. A more careful analysis is needed to establish whether this phase is consistent with an observation of diagonal stripes in $\text{YBa}_2\text{Cu}_3\text{O}_{6.4}$ [52].

The charge and magnetization distribution obtained for the stripe phases stable at $U = 10t$ are shown for both sets of parameters in Fig. 4. In the case of (01) phase realized for the LSCO parameters [Fig. 4(a)], the AF domains consist of three atoms and have almost unreduced charge (15)

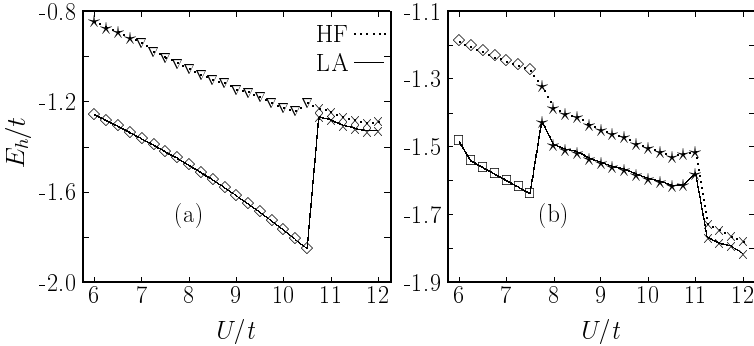


Fig. 3. Energy per doped hole E_h/t in the stable stripe phases (14) obtained in HF (top) and in LA (bottom) method [28]. Part (a) shows stable phases for the parameters of $\text{La}_{2-x}\text{Sr}_x\text{CuO}_4$ ($t' = -0.11t$, $t'' = 0.04t$ [42]): vertical nonmagnetic DW's (\diamond); diagonal AF DW's (∇); vertical DW's with quadrupling of unit cell (\star); and polaron structures with FM intersecting diagonal DW's (\times). Part (b) shows stable phases for the parameters of $\text{YBa}_2\text{Cu}_3\text{O}_{6+x}$ ($t' = -0.30t$, $t'' = 0.20t$ [42]): vertical FM DW's (\square); vertical magnetic DW's with quadrupling of unit cell (\diamond); diagonal FM DW's (\star); and polaron structures with FM intersecting diagonal DW's (\times). Except for polaron structures, all DW's are half-filled.

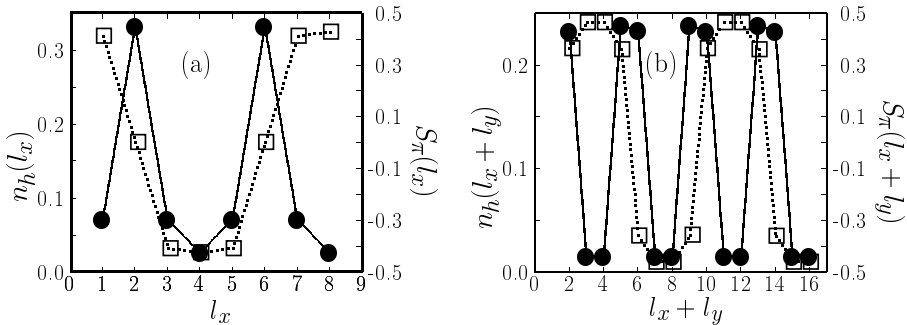


Fig. 4. Charge $n_h(l_x)$ (15) (filled circles) and spin $S_\pi(l_x)$ (16) (open squares) density distributions [28], as obtained for the half-filled (01) and (11) stripes of Fig. 3 at $U = 10t$ for: $\text{La}_{2-x}\text{Sr}_x\text{CuO}_4$ (left) and $\text{YBa}_2\text{Cu}_3\text{O}_{6+x}$ (right).

and magnetization (16) density from the respective values found in the AF insulator at $x = 0$. This state is indeed close to the idealized picture shown in Fig. 1(a). In contrast, the (11) phase obtained for the YBCO parameters [Fig. 4(b)], is somewhat different from Fig. 1(b) — the DW's found from the variational calculation are FM, with two neighboring magnetic moments pointing in the same direction, and in this way give a change of phase in the

staggered magnetization between two AF domains, observed in the variation of $S_\pi(l_x + l_y)$ along the direction perpendicular to the AF domains. It may be expected that more smooth density and magnetization distributions would be obtained, if the LA wave function (9) would be improved by a variational optimization of the density distribution along with the weights of doubly occupied configurations in the correlated ground state.

The examples shown in Figs. 3 and 4, and the results of Ref. [27], demonstrate that local electron correlations beyond the HF states stabilize the half-filled stripe phases in a broad range of parameters. They are consistent with the results obtained in other methods introduced to treat the static correlation effects: the DMRG of White and Scalapino [25], and the mean-field slave-boson technique [26]. Although it has been argued that the long-range Coulomb interactions might help to stabilize the stripe order [26], the evidence has accumulated that the on-site interactions alone suffice to obtain stable half-filled stripe phases [25, 27, 30–33].

4. Dynamical mean-field theory for stripe phases

The case which is most intensely investigated theoretically in the doping by $x = 1/8$ holes, perhaps due to the observation of distinct static stripes in $\text{La}_{1.6-x}\text{Nd}_{0.4}\text{Sr}_x\text{CuO}_4$ [7], which are stable around this hole concentration. However, the stripes occur also away from $x = 1/8$, both in the underdoped and in the overdoped regime [53, 54]. In order to understand the evolution of stripe phases with increasing hole concentration x in the Hubbard model, it is necessary to investigate also other concentrations and look for stable stripe solutions in larger supercells adequate for the underdoped regime. A recent generalization of the DMFT method [32] allows to treat stripe phases, and to address this question in a systematic way.

The central idea of the DMFT is that the dynamical correlations in a fermionic system may be well described by a *local selfenergy* [40]. The *dynamic selfenergy* as a function of ω is then determined self-consistently with the effective medium to which it couples, similar to the conventional mean-field treatment of the Ising model, where a single variable, local magnetization $\langle S^z \rangle$, is determined self-consistently at finite temperature T . Both approaches become exact in infinite spatial dimension $d \rightarrow \infty$: the mean-field theory because the quantum fluctuations vanish in this limit, while the DMFT because the diagrams in the perturbation theory become local [55, 56]. In the past the local form of selfenergy was assumed by neglecting the momentum conservation in second order perturbation theory, and was shown to give very reliable results, capturing more than 95% of the correlation energy in three dimensions [57]. Motivated by this success, here the local selfenergy will be used to describe the dynamics in a 2D model

of doped antiferromagnets. Although this assumption seems to be rather drastic as combining $d = \infty$ with $d = 2$, we argue that the actual qualitative results and a favorable quantitative comparison with some available rigorous properties, justify it *a posteriori*. In fact, it has been shown before that one obtains the correct dispersion and spectral weights of the QP states in the Hubbard model at half-filling ($n = 1$) within the DMFT, if the on-site spin fluctuations and the renormalization of U due to charge fluctuations are included in the local selfenergy [58]. This approach has demonstrated that an accurate treatment of spin and charge fluctuations is necessary to describe correctly the dynamical properties in magnetic phases. Using this experience with the AF Mott insulator, the DMFT method has been recently generalized to treat nonhomogeneous phases with large supercells encountered in stripe phases of HTSO [32], as we present below.

The spectral properties of the Hubbard model (1) may be found from the Green function defined for imaginary time $\tau = it$,

$$G_{mi,nj,\sigma}(\tau) = -\theta(\tau)\langle a_{mi\sigma}(\tau)a_{nj\sigma}^\dagger(0) \rangle + \theta(-\tau)\langle a_{nj\sigma}^\dagger(0)a_{mi\sigma}(\tau) \rangle, \quad (17)$$

which depends on the supercell indices m and n , on the indices within the supercell i and j , and on the spin index σ . Using the periodicity of a stripe phase one finds its Fourier transform, $G_{ij\sigma}(\mathbf{k}, i\omega_\nu)$, which depends of the fermionic Matsubara frequencies $\omega_\nu = (2\nu + 1)\pi T$, with T being a fictitious temperature, playing a role of a low-energy cutoff [40]. Therefore, the Green function is given by an $(L \times L)$ matrix,

$$G_{ij\sigma}^{-1}(\mathbf{k}, i\omega_\nu) = (i\omega_\nu + \mu)\delta_{ij} - h_{ij}(\mathbf{k}) - \Sigma_{i\sigma}(i\omega_\nu)\delta_{ij}, \quad (18)$$

with the site- and spin-dependent *local selfenergy* [40, 55],

$$\Sigma_{i\sigma}(i\omega_\nu) = \Sigma_{i\sigma}^{\text{HF}} + \Sigma_{i\sigma}^{\text{D}}(i\omega_\nu). \quad (19)$$

The selfenergy is labeled by the site index within a stripe supercell, and consists of a HF (static) potential $\Sigma_{i\sigma}^{\text{HF}}$ (4), and a dynamic part $\Sigma_{i\sigma}^{\text{D}}(i\omega_\nu)$, which describes electron correlations and is determined in the DMFT. The kinetic energy $h_{ij}(\mathbf{k})$ in Eq. (18) is obtained for the stripe lattice periodicity with supercells of L atoms as an $(L \times L)$ matrix,

$$h_{ij}(\mathbf{k}) = \sum_n \exp[-i\mathbf{k}(\mathbf{R}_{0i} - \mathbf{R}_{nj})]t_{0i,nj}. \quad (20)$$

For simplicity, we will consider the model (1) with nearest-neighbor hopping only, $t_{0i,nj} = -t$, and thus the matrix (20) has a tridiagonal form.

The local Green functions for each nonequivalent site $i = 1, \dots, L$ are calculated from the diagonal elements of the Green's function matrix (18),

$$G_{i\sigma}(i\omega_\nu) = \frac{1}{N} \sum_{\mathbf{k}} G_{ii\sigma}(\mathbf{k}, i\omega_\nu). \quad (21)$$

The DMFT equations lead thus to a self-consistent problem at site i ,

$$\mathcal{G}_{i\sigma}^0(i\omega_\nu)^{-1} = G_{i\sigma}^{-1}(i\omega_\nu) + \Sigma_{i\sigma}(i\omega_\nu), \quad (22)$$

where $\mathcal{G}_{i\sigma}^0(i\omega_\nu)$ is the effective medium (bath) Green function at site i , which depends on the charge and magnetization density at this site i and, via the bath, on the density distribution at its neighboring sites. In the presence of magnetic order the local Green functions (18) are determined self-consistently together with local HF potentials (4), with the constraint for the total density within the stripe supercell,

$$\frac{1}{L} \sum_{i=1, \sigma}^L n_{i\sigma} = n. \quad (23)$$

This approach to the stripe phase within the DMFT method is therefore analogous to that recently introduced by Potthoff and Nolting for a Mott metal-insulator transition in thin films [59].

The self-consistent problem posed by Eqs. (22) requires the knowledge of both parts of selfenergy (19): (i) the HF part $\Sigma_{i\sigma}^{\text{HF}}$, and (ii) the dynamical part $\Sigma_{i\sigma}^{\text{D}}(i\omega_\nu)$. The latter has to be either derived in a perturbative way by summing up classes of diagrams, or may be determined numerically by solving the correlation problem on a single atom [40]. In the present case the site-dependent selfenergy has been found using an ED algorithm of Caffarel and Krauth [60]. This procedure is motivated by its high accuracy which is especially needed in the magnetic systems, where numerous magnetic phases compete with each other. The main advantage of this method is that it gives unbiased results for the selfenergy and thus includes the leading part of the dynamical processes which are responsible for a many-body behavior of interacting electrons. It is also very well suited to study the ground states of correlated systems, in contrast to quantum Monte-Carlo methods which can provide reliable information only at rather high temperatures ($T \simeq 0.3t$), and therefore cannot be used to investigate the properties of stripe phases. Also the earlier studies of stripe phases based on the perturbative formula for the selfenergy which includes the spin fluctuations appeared to be not accurate enough at low temperatures [61], precisely in the regime where these phases are stable. In fact, the stripes melt at temperatures $T \simeq 70$ K,

and it is therefore difficult to obtain the low temperature limit with sufficient accuracy, when the finite-temperature formalism is used [61].

In the ED method of Caffarel and Krauth a Single-Impurity Anderson Model (SIAM) hybridized with a finite set of orbitals is solved with the Lanczos algorithm at $T = 0$. This non-perturbative approach treats therefore local spin and charge fluctuations exactly, and gives the rigorous form of the selfenergy in the limit of infinite dimension $d \rightarrow \infty$ [40, 56]. In a uniform system a lattice problem is mapped onto an effective SIAM, which is next solved self-consistently with the surrounding lattice. This method is well suited to investigate the spectral properties of stripe phases, when the above mapping is performed independently for each nonequivalent site in a stripe supercell, and leads to L different impurity models for $i = 1, \dots, L$:

$$H_{\text{imp}}^{(i)} = \sum_{\sigma} \left[\epsilon_d c_{i\sigma}^{\dagger} c_{i\sigma} + \sum_{k=1}^{n_s-1} \epsilon_{k\sigma}^{(i)} a_{k\sigma}^{\dagger} a_{k\sigma} + \sum_{k=1}^{n_s-1} \left(V_{k\sigma}^{(i)} a_{k\sigma}^{\dagger} c_{i\sigma} + V_{k\sigma}^{(i)*} c_{i\sigma}^{\dagger} a_{k\sigma} \right) \right] + U n_{i\uparrow} n_{i\downarrow}, \tag{24}$$

with L self-consistency conditions (22). Each impurity model includes $n_s - 1$ effective orbitals labeled by $k = 1, \dots, n_s - 1$, which stand for the conduction band and couple to the impurity atom, where the correlation problem is solved.

Unlike in a real finite cluster, here the conduction-band orbital energies $\epsilon_{k\sigma}^{(i)}$ and the hybridization elements $V_{k\sigma}^{(i)}$ are the effective parameters. In order to start the iteration it is convenient to solve first the noninteracting ($U = 0$) impurity Green function $\mathcal{G}_{i\sigma, n_s}^0(i\omega_{\nu})$, which is given by the following form for atom i ,

$$\mathcal{G}_{i\sigma, n_s}^0(i\omega_{\nu})^{-1} = i\omega_{\nu} - \epsilon_d - \sum_{k=1}^{n_s-1} \frac{\left(V_{k\sigma}^{(i)} \right)^2}{i\omega_{\nu} - \epsilon_{k\sigma}^{(i)}}. \tag{25}$$

The crucial step is the solution of the SIAM for $i = 1, \dots, L$ using the Lanczos algorithm to get the impurity selfenergies $\Sigma_{i\sigma}(i\omega_{\nu})$ which are required for the next cycle. Therefore, the numerical effort increases linearly with the size of the magnetic unit cell L in the stripe phase.

After solving of the effective cluster problem, the local Green functions $G_{i\sigma}(i\omega_{\nu})$ are determined. Self-consistency is implemented by extracting from Eq. (22) the new selfenergy (19), and next Eq. (18) for $G_{ij\sigma}(\mathbf{k}, i\omega_{\nu})$ is used to start the next iteration. Finally, the parameters of the effective SIAM $\{\epsilon_{k\sigma}^{(i)}, V_{k\sigma}^{(i)}\}$ are obtained by fitting the noninteracting problem represented by the bath Green function $\mathcal{G}_{i\sigma}^0(i\omega_{\nu})$ to the actual Green function $\mathcal{G}_{i\sigma, n_s}^0(i\omega_{\nu})$ (25) on the imaginary energy axis, with the latter function obtained for the finite-orbital problem posed by the SIAM. The best choice is obtained by

minimizing the cost function [59,60],

$$\chi_i^2 = \frac{1}{\nu_{\max} + 1} \sum_{\nu=0}^{\nu_{\max}} |\mathcal{G}_{i\sigma, n_s}^0(i\omega_\nu)^{-1} - \mathcal{G}_{i\sigma}^0(i\omega_\nu)^{-1}|, \quad (26)$$

for each impurity problem labeled by i . This method uses a drastic approximation for a conduction band which is represented just by a *finite set* of $n_s - 1$ effective orbitals. Of course, one could reproduce an exact result for an infinite system only in the limit of $n_s \rightarrow \infty$. However, the convergence with the increasing cluster size is very fast, and reliable results for a metal-insulator transition in the Hubbard model could be obtained by solving relatively small clusters with $n_s < 10$ [60]. The convergence is of similar quality also in the present problem, and the results obtained with $n_s = 8$ will be presented in the next Section.

Apart from the static properties such as density (15) and magnetization (16) distribution, the Green functions (18) allow to determine the spectral function,

$$A(\mathbf{k}, \omega) = -\frac{1}{\pi} \frac{1}{LN} \text{Im} \sum_{mi, nj, \sigma} e^{-i\mathbf{k}(\mathbf{R}_{mi} - \mathbf{R}_{nj})} G_{mi, nj, \sigma}(\omega). \quad (27)$$

This quantity will be used below to analyze the mechanism of stability and the momentum dependence of the photoemission spectra in stripe phases.

5. Stripe phases as one-dimensional metals

We will be interested here in a generic picture which follows from the DMFT approach and thus the numerical examples will be limited to the simplest case, to the Hubbard Hamiltonian (1) with nearest-neighbor hopping only. This choice is sufficiently close to the realistic parameters of $\text{La}_{2-x}\text{Sr}_x\text{CuO}_4$ [42]. Stripe phases in the doped Hubbard model were found using the above ED method within the DMFT by an extensive numerical search for self-consistent solutions with the lowest energy, starting from different initial conditions appropriate for various type of polaron and stripe ordering [32]. The finite 8×8 and larger lattices with periodic boundary conditions used for these calculations accommodated always at least eight stripe supercells with the periodic boundary conditions, which are sufficient to approximate the stripe phases stable in the thermodynamic limit. Here we summarize the results obtained for $U = 12t$, a value representative for $\text{La}_{2-x}\text{Sr}_x\text{CuO}_4$ compounds, which reproduces the experimental ratio of $t/J = 3$ [11], with $J = 4t^2/U$. At low doping one might expect isolated polarons which were found before in the HF studies [6, 20]. However, the polarons are unstable in the present DMFT calculations and instead

a uniform AF state with a gradually reduced magnetization in the weakly doped regime of $x < 0.03$ was found. This suggests that the HF approach overestimates the local density changes in the doped systems, and agrees qualitatively with the experimentally observed AF long-range order in the weakly doped regime up to $x \simeq 0.02$, reported for $\text{La}_{2-x}\text{Sr}_x\text{CuO}_4$ [9, 62, 63].

The stripes were found to be stable in a broad range of hole doping $0.03 < x < 0.2$ using the DMFT. The DW's are populated by the doped holes with the filling corresponding to half-filled stripes in the stable phases, but the density distribution is more smooth than in the corresponding HF states corrected by the LA method, for all cases discussed in Sec. 3. First, near the undoped AF Mott insulator, the (11) stripes with large supercells are stabilized for $0.03 < x \leq 0.05$ by a (weak) CDW superimposed with a SDW along the wall. These states have very large supercells consisting typically of ~ 160 atoms, and are characterized by the extended DW's with the clusters of four sites along x axis, $|0\rangle - |\uparrow\rangle - |0\rangle - |\downarrow\rangle$, on each (11) DW itself, and the AF domains between them. They demonstrate a generic tendency towards phase separation within a doped antiferromagnet into hole-poor and hole-rich regions [5], and may be seen as a compromise between the uniform AF order and (01) stripes which occur only at higher doping.

Site-centered vertical stripes, with half-filled DW's, were found to be the most stable structures in a broad range of doping $0.05 < x < 0.17$. The size of AF domains, separated by a line of nonmagnetic atoms, is first large (seven atoms at $x = 1/16$), but shrinks with the increasing doping down to three atoms at $x = 1/8$. Beyond $x = 1/8$ one finds up to $x \simeq 0.17$ a lock-in effect of the same structure with a charge (magnetic) unit cell consisting of four (eight) sites, and the AF domains with three atoms along the x direction. Two examples of the (01) structures stable at $x = 1/12$ and 0.15 are shown in Fig. 5. Although the hole density has distinct maxima at the DW's, the holes are more delocalized than in the HF calculations [6, 19], and in the LA method [27], discussed in Sec. 3. This result agrees with the slave-boson calculations [26], and with numerical DMRG [25], where also more smooth density variations were obtained than in the corresponding HF states. Moreover, the density distribution is quite stable around the DW's in the underdoped regime, with $n_i \simeq 0.850$ and $n_i \simeq 0.830$, at doping $x = 1/16$ and $x = 1/8$, respectively, and a rather small doping at the central sites in the AF domains ($n_i \simeq 0.97$ in the case of $x = 1/16$ shown in Fig. 5). On the contrary, for the doping $x > 1/8$ the hole density increases fast within the AF domains. For instance, $n_i \simeq 0.92$ and 0.88 was found at the central atom in the AF domains for $x = 1/8$ and $x = 0.15$, respectively.

Finally, as a result of increasing hole density within the AF domains and the decreasing amplitude of the SDW shown along the x direction in Fig. 5, at doping $x > 0.17$ kinks and antikinks along the DW's develop,

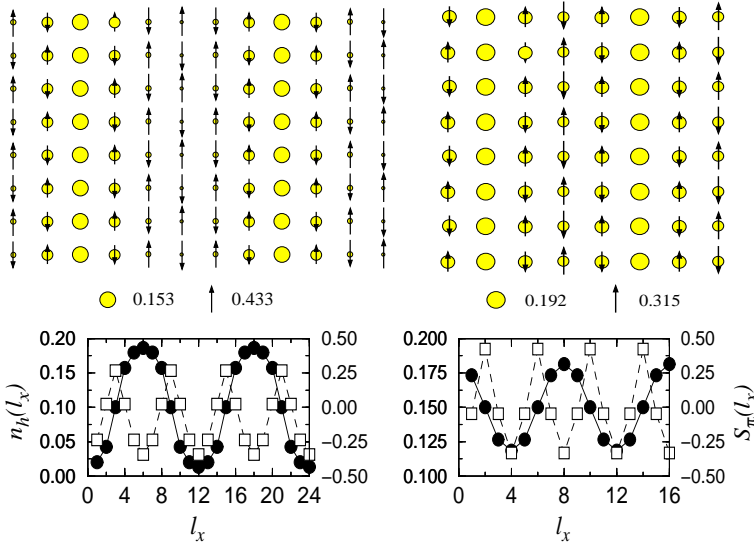


Fig. 5. Vertical site-centered (01) stripe phases obtained in DMFT for $x = 1/12$ (left) and $x = 0.15$ (right) at $U = 12t$ [32]. Top part shows doped hole (circles) and magnetization (arrows) densities; their spatial variations are represented by $n_h(l_x)$ (empty squares) and $S_\pi(l_x)$ (filled circles) in the lower part.

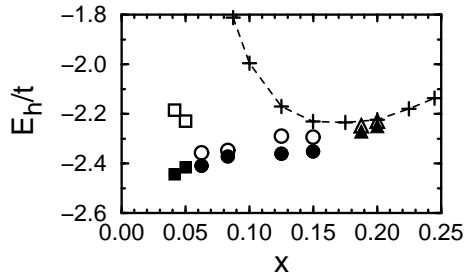


Fig. 6. Energy per doped hole E_h/t in the stable stripe phases (filled symbols), in the respective excited states (empty symbols), and in a uniform paramagnetic phase (pluses), as obtained in DMFT at $U = 12t$. The stable stripe phases are found at $x < 0.20$, as explained in the text: diagonal (11) structures (squares), site-centered (01) stripe phase shown in Fig. 5 (circles), and bond-centered (01) stripe phases (triangles).

the bond-centered (01) stripe phases with pairs of magnetic atoms on the DW's similar to those of White and Scalapino [25] are energetically favored, and the stripe structure gradually melts. This new type of stripe phases, not found in the HF calculations, indicates a smooth crossover from the site-

centered to bond-centered (01) stripes. The gradual transition between three different stripe phases is also seen in the values of energy per one doped hole $E_h^S(x)$, found now from Eq. (14) within the DMFT method (Fig. 6). The energy increases monotonically as a function of doping x , showing that the (11) and (01) stripe phases discussed above are stable against macroscopic phase separation. The energy difference between the site-centered and bond-centered stripe phases is typically small, *e.g.* $\Delta E_h^S \sim 0.05t$ for $x \simeq 1/8$. One observes also a decreasing excitation energy with increasing x which indicates that the stripe phases are gradually destabilized with increasing doping. Therefore, one expects strong transverse stripe fluctuations in the bond-centered phases [64], not included in the DMFT approach, which could stabilize them a bit more against the site-centered stripes. It has been argued that such fluctuations might enhance superconducting correlations in the ground state [65].

In contrast, the energy of the *uniform* paramagnetic phase per one hole, $E_h^P(x)$, determined in a similar way to Eq. (14), has a minimum at $x_m \simeq 0.16$, with $E_h^P(x_m) \simeq -2.23t$ ($-1.94t$) for $U = 12t$ ($U = 8t$). This indicates a generic tendency of this phase towards *phase separation* [5], as a lower energy can be obtained at doping $x < 0.16$ just by separating the sample into hole-poor and hole-rich regimes, following the Maxwell construction. This shows that the stripe phases are a natural consequence of this instability, and the energy per hole found in them $E_h^S(\delta)$ is just somewhat lower than the energy of the paramagnetic phase at its minimum, $E_h^P(x_m)$. Doping beyond x_m soon destabilizes the stripes due to the increasing spin and charge fluctuations, as discussed above, and the energies $E_h^S(x)$ and $E_h^P(x)$ come close to each other and merge above $x = 0.20$. This estimate agrees well with the observed gradual disappearance of charge inhomogeneities in $\text{La}_{2-x}\text{Sr}_x\text{CuO}_4$ above the optimal doping [66].

The stripe superstructure is clearly seen in the charge and spin response as the characteristic maxima of the respective structure factors. Using the same notation as in Eqs. (15) and (16), the charge distribution may be described by the Fourier transform of the static hole-hole correlation function in the reciprocal space,

$$\mathcal{C}(\mathbf{k}) = \frac{1}{LN} \sum_{(l_x, l_y)} e^{-i(k_x l_x + k_y l_y)} \langle 1 - n_{(0,0)} \rangle \langle 1 - n_{(l_x, l_y)} \rangle. \quad (28)$$

For a stripe phase the summation is performed over the 2D lattice of N supercells containing L sites each. Here $\mathbf{k} = (k_x, k_y)$ is a vector from the first Brillouin zone. This function may be measured in elastic X-ray scattering and has characteristic maxima at $\mathbf{Q}_c = (\pm 4\eta\pi, 0)$ for the vertical (01) stripes. In experiment, however, a superposition of (01) and (10)

phases from different CuO_2 planes is observed, and thus the maxima are symmetrically distributed around the $\Gamma = (0,0)$ point at $\mathbf{Q}_c = (\pm 4\eta\pi, 0)$ and $\mathbf{Q}_c = (0, \pm 4\eta\pi)$ (see Fig. 7).

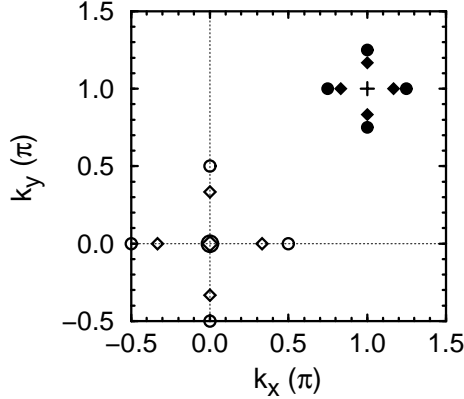


Fig. 7. Maxima of the magnetic structure factor $\mathcal{S}(\mathbf{k})$ (filled symbols) and charge structure factor $\mathcal{C}(\mathbf{k})$ (empty symbols) for the (01)/(10) stripe phases shown in Fig. 5. The peaks obtained for $x = 1/12$ and 0.15 are indicated by diamonds and circles, respectively. Increasing doping x corresponds to the increasing splitting of the neutron (X-ray) peaks in $\mathcal{S}(\mathbf{k})$ [$\mathcal{C}(\mathbf{k})$] with respect to the M (Γ) point.

The neutron scattering measures magnetic correlations in real space which are described by the magnetic structure factor,

$$\mathcal{S}(\mathbf{k}) = \frac{1}{LN} \sum_{(l_x, l_y)} e^{-i(k_x l_x + k_y l_y)} \langle S_{(0,0)}^z \rangle \langle S_{(l_x, l_y)}^z \rangle. \quad (29)$$

Experimentally the stripes were observed as the shift of the neutron peak $\propto \eta$, which moves away from a single AF maximum of $\mathcal{S}(\mathbf{k})$ at the $M = (\pi, \pi)$ point for $x = 0$ to four symmetric points around M (Fig. 7): $\mathbf{Q}_s = [(1 \pm 2\eta)\pi, \pi]$ and $\mathbf{Q}_s = [\pi, (1 \pm 2\eta)\pi]$, if $x > 0$. These two values correspond again to a superposition of (01) and (10) stripe phases. This result shows that the stripes in the cuprates are indeed (10) type, in contrast to the diagonal (11) stripes observed in the nickelates [24]. The value of η was found to be increasing with hole doping x , with $\eta \simeq x$ at $x < 1/8$ [7, 9, 53]. If the magnetic (charge) unit cell decreases with doping x , as reported above, the splitting of the maxima of $\mathcal{S}(\mathbf{k})$ [$\mathcal{C}(\mathbf{k})$] around the M (Γ) point increases.

The DMFT calculations of Ref. [32] give a linear dependence of the neutron peak splitting on doping, $\eta \propto x$, in the range of low doping, $x \leq 1/8$, and a constant value $\eta = 1/8$ for $x > 1/8$ [Fig. 8(a)]. Such a crossover behavior was observed in the experiments of Yamada *et al.* [53], and indicates

a unique stability of half-filled DW's in the (01) stripe phase, as obtained in the HF studies [20]. For the structures with diagonal extended DW's obtained at low doping $x < 0.06$ the maxima of $\mathcal{S}(\mathbf{k})$ found at $\mathbf{Q}_s = [(1 \pm 2\eta_d)\pi, (1 \pm 2\eta_d)\pi]$, with $\eta_d \simeq x/\sqrt{2}$, agree perfectly well with the recent neutron experiments of Wakimoto *et al.* [54]. Although these structures are so different from the (01) phases at higher doping, it is remarkable that the corresponding values of η_d follow the same linear dependence on x .

The analysis of the total density of states obtained by summing up the spectral functions over the Brillouin zone leads to a conclusion that the chemical potential shifts downwards with hole doping, $\Delta\mu \propto -x^2$ [Fig. 8(b)], in agreement with the Monte-Carlo simulations of the 2D Hubbard model [67]. Therefore, the charge susceptibility is enhanced in the limit of $x \rightarrow 0$, reproducing a universal property of the Mott–Hubbard metal-insulator transition [67]. Whether or not this behavior is observed in experiment is still controversial. The data points obtained by Ino *et al.* [39] have rather large error bars, but seem to be instead more consistent with a weak decrease of μ with increasing x in the range of stripe phases $x \leq 0.15$, followed by a quite rapid drop when the stripes start to melt. This might be related to the change of the Fermi surface shape around $x = 0.15$ doping, which violates the Luttinger theorem in the underdoped regime [68]. In any case, the observed behavior indicates that the weakly-doped cuprates are in a regime of anomalous metallic phase, and a direct transition from a Luttinger liquid to a superconductor occurs under decreasing temperature [69]. This non-Fermi liquid regime has numerous consequences for several transport properties of the normal phase [4, 70], which have been observed in the same regime of doping, where the stripe phases are stable in $\text{La}_{2-x}\text{Sr}_x\text{CuO}_4$.

The main advantage of using the DMFT is that it allows also to investigate the spectral functions $A(\mathbf{k}, \omega)$ (27) of the stripe phases. The DMFT gives a strong renormalization of the Mott–Hubbard gap from its HF value, and modifies the structure of the Hubbard subbands. If a single hole is doped, a QP peak is found close to μ , with a dispersion familiar from the t - J model [58]. This dispersion suggests that the hole doping would occur first at the $X = (\pi, 0)$ point, if the QP band remains unchanged under doping, and the Fermi energy enters the LHB. On the contrary, the low-energy spectral properties at $\omega \simeq \mu$ are determined by the many-body processes in the doped Hubbard model, and by the spectral weight transferred from the UHB [44]. Therefore, the obtained photoemission spectra (for $\omega \leq \mu$) at low doping x consist of two distinct features: the incoherent part of the LHB, extending in a range of $-6t < \omega - \mu < -2t$, with a large intensity around $\omega - \mu \simeq -4.8t$, and a QP part in a range of $-0.7t < \omega - \mu < 0$. The latter dispersive feature is clearly seen in Fig. 9; it is similar to that found for a single hole [58], has a dispersion $\sim 2J$ (here $J/t = 4t/U = 1/3$), and comes

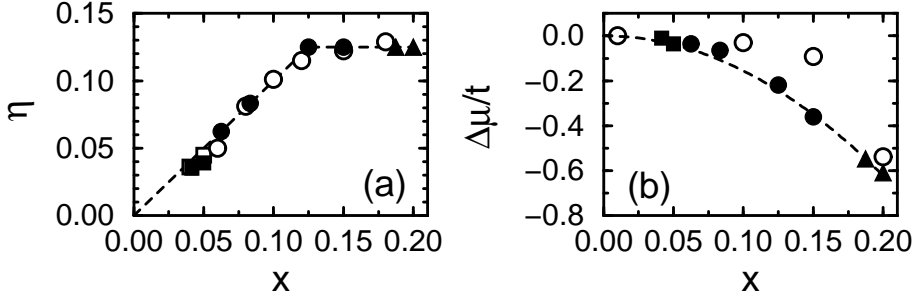


Fig. 8. Evolution of the stripe phases with increasing hole doping x , as found in DMFT with $U = 12t$: (a) shift η of the maxima of the magnetic structure factor $S(\mathbf{k})$, and the data points of Yamada *et al.* [53] (empty circles) and Wakimoto *et al.* [54] (empty squares); (b) shift of the chemical potential $\Delta\mu/t$ (points) and the quadratic fit $\Delta\mu/t = a\delta^2$ with $a = -15.57$ (dashed line), and the experimental data of Ino *et al.* [39] for $t = 0.25$ eV (empty circles). Filled symbols show: diagonal (11) SDW stripes with $\mathbf{Q}_s = [(1 \pm \sqrt{2}\eta)\pi, (1 \pm \sqrt{2}\eta)\pi]$ (squares), and vertical (01) site-centered (circles) and bond-centered (triangles), with $\mathbf{Q}_s = [(1 \pm 2\eta)\pi, \pi]$.

close to μ at the X point, but stays well below μ at the remaining points of the AF Brillouin zone, and along the $Y-\Gamma$ and $\Gamma-S$ directions. Due to the stripe superstructure one finds that the directions $\Gamma-X$ and $\Gamma-Y$ are nonequivalent.

The states at $\omega - \mu > 0$ are quite different. Here one finds a large dispersion $\sim 2t$ between the points which belong to the boundary of the AF Brillouin zone (X , Y , and S) and the M point. This large dispersion is reminiscent of the free propagation along the DW's given by Eq. (8), but is now strongly renormalized by the many-body processes: the dispersion along the $X-M$ direction is reduced by a factor close to two, while a similar dispersion occurs as well along the $Y-M$ direction, in spite of its absence in the free 1D band (8). A particularly interesting situation is observed near the X point, where the quasi-1D electronic structure of the site-centered (01) stripe phase merges with the QP band below μ , and gives a *flat band* around the X point. The spectral weight stays *below* μ at the X point, while it crosses the Fermi energy μ just at the $\mathbf{k} = (\pi, \pi/4)$ point, as for a quarter-filled 1D band (8). Remarkably, both features were observed in recent angle-resolved photoemission (ARPES) experiments [34–36]. On the contrary, the free 1D band (8) cannot contribute at the Y point [37], and one observes a gap between the spin-polaron QP band with dispersion $\sim 2J$, and the states at $\omega - \mu > 0$. Also along the $\Gamma-M$ direction the spectra change drastically from those found in a one-particle approach. At the $\mathbf{k} = (\pi/4, \pi/4)$ point, where [as at $\mathbf{k} = (0, \pi/4)$] the 1D band would cross

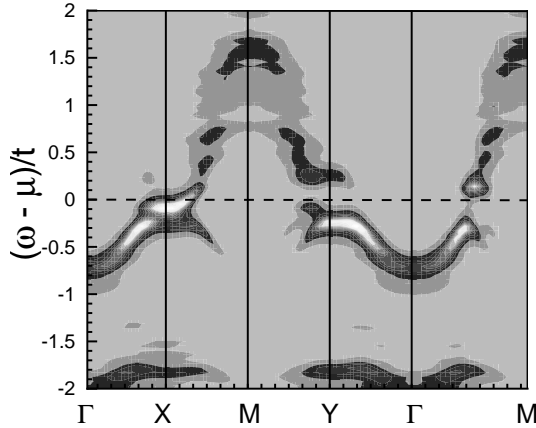


Fig. 9. Spectral function $A(\mathbf{k}, \omega)$ of the stripe phase at $x = 1/12$ with $U = 12t$, as obtained along the main directions of the 2D Brillouin zone, with $\Gamma = (0, 0)$, $X = (\pi, 0)$, $Y = (0, \pi)$, $M = (\pi, \pi)$, and $S = (\pi/2, \pi/2)$ [32].

the Fermi energy, almost no spectral weight is found. Instead, a spin-polaron QP appears around this point, still well below μ , but approaching the Fermi energy along the Γ - S direction. At the S point itself the QP stays well below μ , and no spectral weight appears at the Fermi level, giving again a gap between the occupied and unoccupied part of the LHB. This behavior agrees quantitatively with the observed ARPES spectra for $\text{La}_{2-x}\text{Sr}_x\text{CuO}_4$ [35, 36] and $\text{La}_{1.28}\text{Nd}_{0.6}\text{Sr}_{0.12}\text{CuO}_4$ [34].

At higher doping $x \simeq 0.15$ essentially a similar picture is obtained (Fig. 10), supporting the view that the spin-polaron QP band arising from

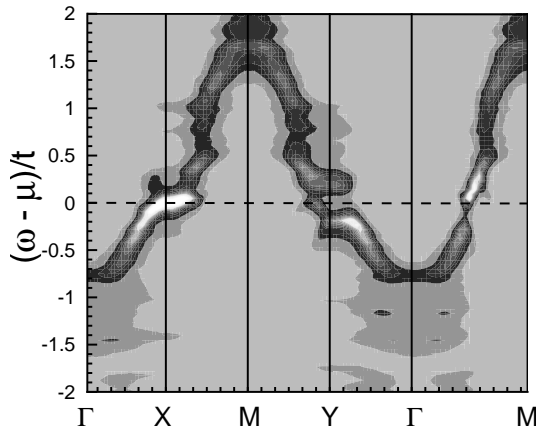


Fig. 10. Spectral function $A(\mathbf{k}, \omega)$ of the stripe phase at $x = 0.15$ ($U = 12t$) [32].

a hole moving in an AF domain, and the renormalized 1D-band above μ are universal as long as the (01) stripes remain stable structures. The differences to the low-doping regime are of quantitative nature only. First of all, the flat QP at the X point moves to the Fermi level when the filling of the DW's increases beyond half filling in the range of doping $x > 1/8$. The large spectral weight at the X point gives also some 'shadows' at the Y and S points, but the gaps are still seen at the latter two points. The feature above μ has a larger spectral weight and resembles a band with a similar dispersion along the X - M and X - M direction.

By integrating the spectra over the Brillouin zone, one finds a density of states with a pseudogap at the Fermi level. This pseudogap is pinned to μ when the hole doping x increases, and the (01) stripes become more dense. It may be therefore considered to be the reason of stability of the (01) stripe structures beyond the HF picture. Indeed, this pseudogap is gradually filled by spectral weight, and finally disappears when the stripe order melts with increasing hole doping x . One could attempt to understand the results of the DMFT by simulating the electronic structure in HF, using the magnetic potentials (4). In contrast to the HF approximation, however, the value of the Coulomb interaction U does not remain constant in the DMFT, but is renormalized by the local dynamics to a value [71, 72],

$$\bar{U}_i = \frac{U}{1 + U\chi_i^{pp}(0)}, \quad (30)$$

where the particle-particle vertex χ_i^{pp} is determined by the Weiss field,

$$\chi_i^{pp}(0) = (k_B T) \sum_{\mu} \mathcal{G}_{i\uparrow}^0(i\omega_{\mu}) \mathcal{G}_{i\downarrow}^0(-i\omega_{\mu}). \quad (31)$$

Therefore, one can analyze the electronic structure of tight-binding electrons moving on a 2D lattice within a site-dependent magnetic potential $\propto \bar{U}_i$ which corresponds to the stripe structure,

$$H = -t \sum_{mi, nj, \sigma} a_{mi\sigma}^{\dagger} a_{nj\sigma} - \sum_{mi} e^{i\mathbf{Q}\mathbf{R}_{mi}} V_{mi} (n_{mi\uparrow} - n_{mi\downarrow}), \quad (32)$$

using the same notation as in Eq. (1). Local magnetic potentials

$$V_{(i_x, i_y)} \equiv e^{i\mathbf{Q}\mathbf{R}_{(i_x, i_y)}} \bar{U}_{(i_x, i_y)} |\langle S_{(i_x, i_y)}^z \rangle|, \quad (33)$$

alternate due to the phase factor $e^{i\mathbf{Q}\mathbf{R}_{(i_x, i_y)}}$ when i_y is varied for vertical (01) stripe phases, with $\mathbf{Q} = [(1 \pm 2\eta)\pi, \pi]$. These potentials may be treated as external parameters, and the electronic structure of the (01) phases is

then parametrized by a set of values $\{V_{i_x}\}$, with $V_0 = 0$. They play a crucial role and determine whether the system is *metallic* or *insulating*. Let us label by V_1 and V_2 the potentials at the first and second neighbors of the DW, respectively. It has been found by the numerical analysis that the photoemission weight vanishes at μ for the $\mathbf{k} = (\pi/4, \pi/4)$ point and a gap opens, if a condition for the potentials close to the DW, $V_2 \geq 2V_1$, is satisfied [32]. Indeed, the magnetic potentials change so rapidly in the weakly doped regime $x < 1/8$, but not for large doping $x > 1/8$; for instance at $x = 1/12$ the spin densities found in the DMFT and the renormalized values of \bar{U}_i lead to $V_2 \simeq 2.07t$ and $V_1 \simeq 0.99t$. The strong renormalization of spin (and charge) densities next to the DW's with respect to the HF values is due to charge fluctuations included in the DMFT, and demonstrates that local correlations are responsible for the ARPES spectra observed in HTSO [34–36].

6. Summary and open problems

The presented results of the calculations performed beyond the HF approximation: the LA method for the ground state [27], and the DMFT both for the ground state and for the spectral properties [32], demonstrate that the correlation effects are of crucial importance, and are observed in the ARPES spectra $\text{La}_{2-x}\text{Sr}_x\text{CuO}_4$ at low and intermediate doping. It is quite remarkable that the sequence of stripe phases, with (11) stripes followed by (01) stripes, the latter with decreasing and then constant size of the AF domains under increasing hole doping x , could be obtained within the DMFT calculations, in perfect agreement with the experimental findings.

While the tendency towards charge and spin separation in a form of stripe phases may be understood as a compromise which follows from optimizing the kinetic energy $\propto t$ and the magnetic energy $\propto J$ at the same time, the detailed mechanism of this instability is still under investigation. First of all, the HF studies have clarified that the largest kinetic energy gains are obtained due to the hopping elements t_\perp *perpendicular* to the (01) stripes by the solitonic mechanism [20], while the elements t_\parallel *parallel* to the (01) stripes are less important for their stability. Therefore, it may be expected that the stripe ordering will always tune the direction of the DW's along a weaker hopping in the anisotropic model, realizing the condition $t_\perp > t_\parallel$, and indeed this trend was confirmed by recent numerical simulations within the t - J model [73]. In contrast, there are more parallel AF bonds than perpendicular to the direction of the (nonmagnetic) DW's, and therefore an increasing superexchange *parallel* to the DW's J_\parallel will have a stabilizing effect on the (01) stripes. The situation concerning the (11) stripes is not yet explored — in order to demonstrate the universality of the above mechanism

it would be worthwhile to show that here the second neighbor hopping t' across the (11) stripes and exchange elements J' along them would have similar effects on the stability of the (11) stripe phase.

It is quite remarkable that the spectral functions obtained for the (01) stripe phases in the DMFT have only a very weak relation to the HF band structure, but are similar to the experimental observations. The spectra discussed in Sec. 5 show an interesting superposition of the spin-polaron QP states with a dispersion of $\sim 2J$, and a broader dispersion of the states above μ , suggested by a 1D metallic behavior *along* the nonmagnetic DW's. Such experimental features at low energies $|\omega - \mu| < J$ as: (i) no significant spectral weight at the $\Gamma = (0, 0)$ point; (ii) flat QP state at the $X = (\pi, 0)$ point, and its absence at the $Y = (\pi, 0)$ point, leading to a still distinct flat structures at both these points when the (01) and (10) stripes contribute with equal intensity in experiment; (iii) also significant, but dispersive and weaker QP state at $S = (\pi/2, \pi/2)$ point, with a distinct gap separating the photoemission ($\omega < \mu$) and inverse photoemission ($\omega > \mu$) part, agree well with the experimental observations [34–36].

The low-energy spectral weights obtained in photoemission at the X [$\mathbf{k} = (\pi, 0)$] and S [$\mathbf{k} = (\pi/2, \pi/2)$] points are shown below the phase diagram of Fig. 11. While the weight at the X point gradually increases with increasing hole concentration x , it vanishes at the S point below $x = 1/8$, and only in the regime of $x > 1/8$ the gap at this point is gradually filled. In contrast, the gap does not open at the S point in the weakly doped regime of $\text{Bi}_2\text{Sr}_2\text{CaCu}_2\text{O}_{8+y}$, where a sharp peak is observed at μ both in underdoped and overdoped compounds [74]. Our results show that this difference follows from the static stripes which stabilize only in $\text{La}_{2-x}\text{Sr}_x\text{CuO}_4$, but not in $\text{Bi}_2\text{Sr}_2\text{CaCu}_2\text{O}_{8+y}$. Note that the decrease of the spectral weight of the LHB in the superconducting phase (SC) shown in Fig. 11 is exaggerated, and a weaker dependence on x was derived by analyzing the strongly correlated regime of the Hubbard model [44].

The phenomenon of stripe melting in the $x > 1/8$ doping regime is very intriguing. Increasing hole density enhances the quantum fluctuations and delocalizes the site-centered stripes, producing instead bond-centered stripes [32], and more units of bond-centered stripes are likely to be generated as the stripes become more dynamic. Recently it has been argued that the photoemission experiments should be able to distinguish between both types of (01) stripes, and the ARPES results around $x = 1/8$ doping in $\text{La}_{2-x}\text{Sr}_x\text{CuO}_4$ suggest that the site-centered stripes are observed. It is not very likely, however, that such experiments would help to understand the stripe melting, as the phenomenon is dynamic by itself, and experimental resolution might not be sufficient. Enhanced density of doped holes in the regime of stripe melting could promote the ordering of kinks, caus-

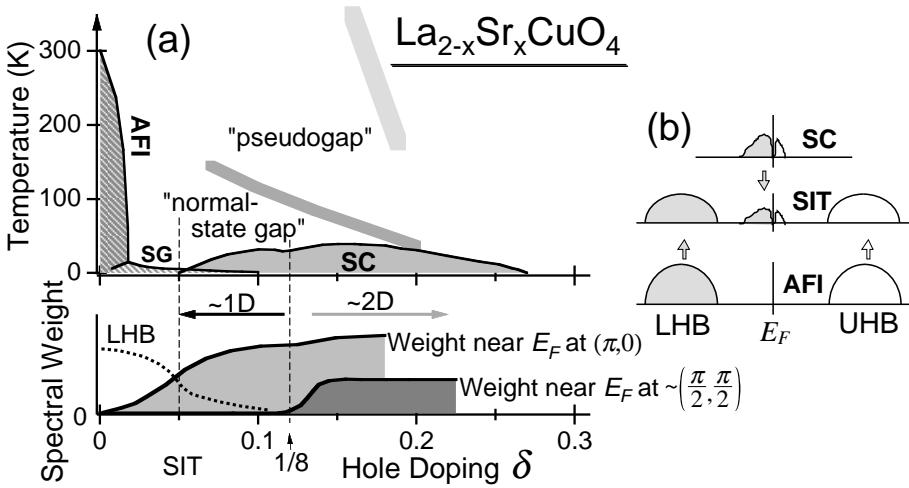


Fig. 11. Part (a): Schematic phase diagram of $\text{La}_{2-x}\text{Sr}_x\text{CuO}_4$ compounds (top), and the evolution of spectral weight with hole doping in the LHB at $\mathbf{k} = (\pi, 0)$ and $\mathbf{k} = (\pi/2, \pi/2)$ [36]. Part (b) shows in a schematic way the modification of spectral weight distribution from an AF Insulator (AFI) around a semiconductor-metal transition (SIT) to a stripe phase with 1D conductivity, or to a superconductor (SC). This figure was obtained due to the courtesy of A. Ino.

ing the stripe phase to tilt. Such states, unlike the instability towards the bond-ordered stripes, are observable in neutron scattering as tilting of the maxima of $\mathcal{S}(\mathbf{k})$ away from the (10) and (01) directions in the reciprocal space [75]. Indeed, such tilted DW's were recently observed in a number of cuprates [63, 76].

Summarizing, we have shown that the instability towards stripe phases, found first in the HF studies [6], is robust and not only survives when the electron correlation effects are treated explicitly, but gives results which agree with experiments. The qualitative physics established by the HF studies applies in a broad range of parameters, also when the Hubbard model is extended either by a further neighbor hopping terms, or to a charge-transfer model. These extensions should be further explored in the future studies in order to clarify the tendency towards stripe formation in different classes of HTSO. Although it has been shown in Sec. 3 that the second neighbor hopping t' may change the most stable structures from (01) to (11) stripes, this point was not yet studied in more sophisticated methods, such as the DMFT. In this context, it would be of interest to derive the parameters of the effective Hubbard model for the electron doped cuprates and to study the relevant regime in order to understand better whether indeed the stripe

instabilities in this class of cuprates are closer to those observed in the nickelates, as claimed recently [23].

The possible role of stripes in the phenomenon of superconductivity is puzzling. The static stripes are stable only in the normal phase of $\text{La}_{2-x}\text{Sr}_x\text{CuO}_4$ compounds [Fig. 11(a)], where the values of T_c are lowest. This alone suggests that the stripe instability competes with the superconducting instability, but it might also be that the fluctuating stripes are different, and support the superconducting fluctuations in a quantum string liquid [77]. The stable stripes in the normal phase of $\text{La}_{2-x}\text{Sr}_x\text{CuO}_4$ give a pseudogap in the density of states [Fig. 11(b)], while a pseudogap was observed in practically all the HTSO, where it explains the transport and thermodynamic properties in the high-temperature regime [11, 70]. As the pseudogap is so universal, it would be interesting to understand better its origin in those situations where static stripes could not be observed so far.

As the most important conclusion of the DMFT studies [32], the vertically (or horizontally) ordered *stripe phases are metallic* along the direction of the nonmagnetic DW's, in contrast to the HF stripes which are always insulating, with a small gap at the Fermi level. The HF gap is smeared out into a *pseudogap* by the dynamical fluctuations which occur due to the coupling of the holes moving along the stripes to spin fluctuations within the AF domains.

It is a pleasure to thank Marcus Fleck and Jan Zaanen for a friendly collaboration and for numerous stimulating discussions, and A. Ino for his agreement for presenting Fig. 11 in the present paper. Valuable discussions with O.K. Andersen, A.I. Lichtenstein, B. Normand, and K. Rościszewski are also kindly acknowledged. This work was supported by the Polish State Committee for Scientific Research (KBN), Project No. 2 P03B 055 20.

REFERENCES

- [1] M. Imada, A. Fujimori, Y. Tokura, *Rev. Mod. Phys.* **70**, 1039 (1998).
- [2] N.F. Mott, *Metal-Insulator Transitions*, Taylor and Francis, London, Philadelphia, 1990.
- [3] A.M. Oleś, M. Cuoco, N.B. Perkins, *Lectures on the Physics of Highly Correlated Electron Systems IV*, edited by F. Mancini, *AIP Conf. Proc.*, Vol. **527**, New York 2000.
- [4] C.M. Varma, P.B. Littlewood, S. Schmitt-Rink, E. Abrahams, A.E. Ruckenstein, *Phys. Rev. Lett.* **63**, 1996 (1989); O. Parcollet, A. Georges, *Phys. Rev.* **B59**, 5341 (1999); V.J. Emery, E. Fradkin, S.A. Kivelson, T.C. Lubensky, *Phys. Rev. Lett.* **85**, 2160 (2000).
- [5] V.J. Emery, S.A. Kivelson, H.Q. Lin, *Phys. Rev. Lett.* **64**, 475 (1990); V.J. Emery, S.A. Kivelson, *Physica* **C209**, 597 (1993).

- [6] J. Zaanen, O. Gunnarsson, *Phys. Rev.* **B40**, 7391 (1989).
- [7] J.M. Tranquada, B.J. Sternlieb, J.D. Axe, Y. Nakamura, S. Uchida, *Nature* **375**, 561 (1995); J.M. Tranquada *et al.*, *Phys. Rev.* **B54**, 7489 (1996).
- [8] J. Zaanen, A.M. Oleś, *Phys. Rev.* **B37**, 9423 (1988).
- [9] M.A. Kastner, R.J. Birgeneau, G. Shirane, Y. Endoh, *Rev. Mod. Phys.* **70**, 897 (1998).
- [10] K.A. Chao, J. Spałek, A.M. Oleś, *J. Phys. C* **10**, L271 (1977).
- [11] E. Dagotto, *Rev. Mod. Phys.* **66**, 763 (1994); J. Jaklič, P. Prelovšek, *Adv. Phys.* **49**, 1 (2000).
- [12] Y. Nagaoka, *Phys. Rev.* **147**, 392 (1966).
- [13] P. Prelovšek, X. Zotos, *Phys. Rev.* **B47**, 5984 (1993); P. Prelovšek, I. Sega, *Phys. Rev.* **B49**, 15241 (1994).
- [14] C. Nayak, F. Wilczek, *Phys. Rev. Lett.* **78**, 2465 (1997).
- [15] J. Zaanen, *J. Phys. Chem. Solids* **59**, 1769 (1998).
- [16] T. Mizokawa, A. Fujimori, *Phys. Rev. Lett.* **80**, 1320 (1998).
- [17] T. Tohyama, S. Nagai, Y. Shibata, S. Maekawa, *Phys. Rev. Lett.* **82**, 4910 (1999).
- [18] M. Vojta, S. Sachdev, *Phys. Rev. Lett.* **83**, 3916 (1999).
- [19] D. Poilblanc, T.M. Rice, *Phys. Rev.* **B39**, 9749 (1989); M. Kato, K. Machida, H. Nakanishi, M. Fujita, *J. Phys. Soc. Jpn.* **59**, 1047 (1990); M. Inui, P.B. Littlewood, *Phys. Rev.* **B44**, 4415 (1991); J.A. Vergés, F. Guinea, E. Louis, *Phys. Rev.* **B46**, 3562 (1992).
- [20] J. Zaanen, A.M. Oleś, *Ann. Phys. (Leipzig)* **5**, 224 (1996).
- [21] E.H. Viertiö, T.M. Rice, *J. Phys.: Condens. Matter* **6**, 7091 (1994).
- [22] J. Zaanen, P.B. Littlewood, *Phys. Rev.* **B50**, 7222 (1994); T. Mizokawa, A. Fujimori, *Phys. Rev.* **B56**, 11 920 (1997); Z.G. Yu, J. Zang, J.T. Gammel, A.R. Bishop, *Phys. Rev.* **B57**, R3241 (1998).
- [23] A. Sadori, M. Grilli, *Phys. Rev. Lett.* **84**, 5375 (2000).
- [24] J.M. Tranquada, D.J. Buttrey, V. Sachan, J.E. Lorenzo, *Phys. Rev. Lett.* **73**, 1003 (1994); J.M. Tranquada, J.E. Lorenzo, D.J. Buttrey, V. Sachan, *Phys. Rev.* **B52**, 3581 (1995).
- [25] S.R. White, D. Scalapino, *Phys. Rev. Lett.* **80**, 1272 (1998); S.R. White, D. Scalapino, *Phys. Rev. Lett.* **81**, 3227 (1998); S.R. White, D. Scalapino, *Phys. Rev.* **B61**, 6320 (2000).
- [26] G. Seibold, E. Sigmund, V. Hiznyakov, *Phys. Rev.* **B57**, 6937 (1998); G. Seibold, C. Castellani, C. Di Castro, M. Grilli, *Phys. Rev.* **B58**, 13 506 (1998).
- [27] D. Góra, K. Rościszewski, A.M. Oleś, *Phys. Rev.* **B60**, 7429 (1999).
- [28] D. Góra, K. Rościszewski, A.M. Oleś, *Acta Phys. Pol.* **A97**, 225 (2000).
- [29] C. Buhler, S. Yunoki, A. Moreo, *Phys. Rev. Lett.* **84**, 2690 (2000).
- [30] A.L. Chernyshev, A.H. Castro Neto, A.R. Bishop, *Phys. Rev. Lett.* **84**, 4922 (2000).

- [31] P. Wróbel, R. Eder, *Phys. Rev.* **B62**, 4048 (2000).
- [32] M. Fleck, A.I. Lichtenstein, E. Pavarini, A.M. Oleś, *Phys. Rev. Lett.* **84**, 4962 (2000).
- [33] M.G. Zacher, R. Eder, E. Arrigoni, W. Hanke, *Phys. Rev. Lett.* **85**, 2585 (2000).
- [34] X.J. Zhou, P. Bogdanov, S.A. Kellar, T. Noda, H. Eisaki, S. Uchida, Z. Husain, Z.-X. Shen, *Science* **286**, 268 (1999).
- [35] A. Ino, C. Kim, T. Mizokawa, Z.-X. Shen, A. Fujimori, M. Takaba, K. Tamasaku, H. Eisaki, S. Uchida, *J. Phys. Soc. Jpn.* **68**, 1496 (1999).
- [36] A. Ino, C. Kim, M. Nakamura, T. Yosida, T. Mizokawa, Z.X. Shen, A. Fujimori, T. Kakeshita, H. Eisaki, S. Uchida, *Phys. Rev.* **B62**, 4137 (2000).
- [37] R.S. Markiewicz, *Phys. Rev.* **B62**, 1252 (2000).
- [38] J. Eroles, G. Ortiz, A.V. Balatsky, A.R. Bishop, *Europhys. Lett.* **50**, 540 (2000).
- [39] A. Ino, T. Mizokawa, A. Fujimori, K. Tamasaku, H. Eisaki, S. Uchida, T. Kimura, T. Sasagawa, K. Kishio, *Phys. Rev. Lett.* **79**, 2101 (1997).
- [40] A. Georges, G. Kotliar, W. Krauth, M.J. Rozenberg, *Rev. Mod. Phys.* **68**, 13 (1996).
- [41] J.H. Jefferson, H. Eskes, L.F. Feiner, *Phys. Rev.* **B45**, 7959 (1992); L.F. Feiner, J.H. Jefferson, R. Raimondi, *Phys. Rev.* **B53**, 8751 (1996).
- [42] O.K. Andersen, A.I. Liechtenstein, O. Jepsen, F. Paulsen, *J. Phys. Chem. Solids* **56**, 1573 (1995).
- [43] A.M. Oleś, J. Spalek, *Z. Phys.* **B44**, 177 (1981).
- [44] H. Eskes, A.M. Oleś, *Phys. Rev. Lett.* **73**, 1279 (1994); H. Eskes, A.M. Oleś, M. Meinders, W. Stephan, *Phys. Rev.* **B50**, 17980 (1994).
- [45] C.L. Kane, P.A. Lee, N. Read, *Phys. Rev.* **B39**, 6880 (1989); G. Martínez, P. Horsch, *Phys. Rev.* **B44**, 317 (1991).
- [46] M.I. Salkola, V.J. Emery, S.A. Kivelson, *Phys. Rev. Lett.* **77**, 155 (1996).
- [47] N. Saini, J. Avilla, A. Bianconi, A. Lanzara, M.C. Ascensio, S. Tajima, G.D. Gu, N. Koshizuka, *Phys. Rev. Lett.* **79**, 3467 (1997); Z.-X. Shen, P.J. White, D.L. Feng, C. Kim, G.D. Gu, H. Ikeda, R. Yoshizaki, N. Koshizuka, *Science* **280**, 259 (1998).
- [48] S.I. Matveenko, S.I. Mukhin, *Phys. Rev. Lett.* **84**, 6066 (2000).
- [49] A.M. Oleś, *Phys. Rev.* **B23**, 271 (1981); G. Stollhoff, P. Thalmeier, *Z. Phys.* **B43**, 13 (1981); A.M. Oleś, *Phys. Rev.* **B28**, 327 (1983); A.M. Oleś, G. Stollhoff, *Phys. Rev.* **B29**, 314 (1984).
- [50] M.C. Gutzwiller, *Phys. Rev.* **137**, A1726 (1965).
- [51] G. Stollhoff, P. Fulde, *J. Chem. Phys.* **73**, 4548 (1980); G. Stollhoff, *J. Chem. Phys.* **105**, 227 (1996).
- [52] P. Dai, H.A. Mook, F. Dogan, *Phys. Rev. Lett.* **80**, 1738 (1998).
- [53] K. Yamada *et al.*, *Phys. Rev.* **B57**, 6165 (1998).

- [54] S. Wakimoto *et al.*, *Phys. Rev.* **B60**, R769 (1999); S. Wakimoto *et al.*, *Phys. Rev.* **B61**, 3699 (2000).
- [55] W. Metzner, D. Vollhardt, *Phys. Rev. Lett.* **62**, 324 (1989).
- [56] D. Vollhardt, in: *Correlated Electron Systems*, edited by V.J. Emery, World Scientific, Singapore 1993, p. 57.
- [57] G. Tréglia, F. Ducastelle, D. Spanjaard, *J. Phys. (Paris)* **41**, 281 (1980); G. Tréglia, F. Ducastelle, D. Spanjaard, *Phys. Rev.* **B21**, 3729 (1980).
- [58] M. Fleck, A.I. Lichtenstein, A.M. Oleś, L. Hedin, V.I. Anisimov, *Phys. Rev. Lett.* **80**, 2393 (1998); M. Fleck, A.I. Lichtenstein, A.M. Oleś, L. Hedin, *Phys. Rev.* **B60**, 5224 (1999).
- [59] M. Potthoff, W. Nolting, *Eur. Phys. J.* **B8**, 555 (1999).
- [60] M. Caffarel, W. Krauth, *Phys. Rev. Lett.* **72**, 1545 (1994).
- [61] M. Fleck, A.I. Lichtenstein, A.M. Oleś, in: *High Temperature Superconductivity*, edited by S. E. Barnes, J. Ashkenazi, J.L. Cohn, and F. Zuo, *AIP Conf. Proc.*, Vol. **483**, New York 2000, p. 45.
- [62] C. Niedermayer, C. Bernhard, T. Blasius, A. Golnik, A. Moodenbaugh, J.I. Budnick, *Phys. Rev. Lett.* **80**, 3843 (1998); H.-H. Klauss, W. Wagener, M. Hillberg, W. Kopmann, H. Walf, F.J. Litterst, M. Hücker, B. Büchner, *Phys. Rev. Lett.* **85**, 4950 (2000).
- [63] S. Wakimoto, S. Ueki, Y. Endoh, K. Yamada, *Phys. Rev.* **B62**, 3547 (2000).
- [64] J. Tworzydło, O.Y. Osman, C. van Duin, J. Zaanen, *Phys. Rev.* **B59**, 115 (1999).
- [65] V.J. Emery, S.A. Kivelson, O. Zachar, *Phys. Rev.* **B56**, 6120 (1997).
- [66] E.S. Božin, G.H. Kwei, H. Takagi, S. Billinge, *Phys. Rev. Lett.* **84**, 5856 (2000).
- [67] N. Furukawa, M. Imada, *J. Phys. Soc. Jpn.* **62**, 2557 (1993).
- [68] C. Gröber, R. Eder, W. Hanke, *Phys. Rev.* **B62**, 4336 (2000).
- [69] A.H. Castro Neto, F. Guinea, *Phys. Rev. Lett.* **80**, 4040 (1998).
- [70] T. Timusk, B. Statt, *Rep. Prog. Phys.* **62**, 61 (1999).
- [71] L. Chen, C. Bourbonnais, T. Li, A.M.S. Tremblay, *Phys. Rev. Lett.* **66**, 369 (1991); Y.M. Vilks, A.M.S. Tremblay, *J. Phys. I (France)* **7**, 1309 (1997).
- [72] M. Fleck, A.M. Oleś, L. Hedin, *Phys. Rev.* **B56**, 3159 (1997).
- [73] B. Normand, private communication, 2000.
- [74] Z.-X. Shen, W.E. Spicer, D.M. King, D.S. Dessau, B.O. Wells, *Science* **267**, 343 (1995); D.S. Marschall *et al.*, *Phys. Rev. Lett.* **76**, 4841 (1996); H. Ding *et al.*, *Phys. Rev. Lett.* **76**, 1533 (1996).
- [75] M. Bosch, W. van Saarloos, J. Zaanen, *Physica* **C340**, in press (2000).
- [76] H. Kimura *et al.*, *Phys. Rev.* **B59**, 6517 (1999); Y.S. Lee, R.J. Birgeneau, M.A. Kastner, Y. Endoh, S. Wakimoto, K. Yamada, R.W. Erwin, S.-H. Lee, G. Shirane, *Phys. Rev.* **B60**, 3643 (1999).
- [77] H. Eskes, O.Y. Osman, R. Grimberg, W. van Saarloos, J. Zaanen, *Phys. Rev.* **B58**, 6963 (1998).